International Journal of Multidisciplinary Research and Development
Online ISSN: 2349-4182 Print ISSN: 2349-5979, Impact Factor: RJIF 5.72
www.allsubjectjournal.com
Volume 3; Issue 5; May 2016; Page No. 232-241

Hall effects and magnetic field effects on flow past a parabolic accelerated isothermal vertical plate with uniform mass diffusion in the presence of Thermal radiation

[1] Lakshmi Velu, [2] Muthucumaraswamy Rajamanickam
[1] Department of Mathematics, Rajalakshmi Engineering College, Thandalam, Sriperumbudur 602 105, Tamil Nadu, India
[2] Department of Applied Mathematics, Sri Venkateswara College of Engineering, Pennalur, Sriperumbudur 602105, Tamil Nadu, India,

Abstract
The objective of this paper is to investigate the heat and mass transfer effects on flow past an parabolic accelerated isothermal infinite vertical plate in the presence of thermal radiation, magnetic field and hall effect. The non-linear, coupled partial differential equations for momentum, mass and energy together with boundary conditions are reduced to dimensionless form. Exact solutions of the governing equations are obtained using the Laplace transform technique. The numerical results for the velocity, the temperature profiles and concentration profiles were presented graphically. The flow phenomenon has been characterized with the help of flow parameters such as hall parameter (m), Hartmann number (M), rotation parameter (Ω), Schmidt number (Sc), Prandtl number (Pr), Grashof number for heat and mass transfer (Gr, Gc).An imposed rotation parameter Ω satisfying $\Omega = \frac{M^2 m}{1+m^2}$, the transverse motion (transverse to main flow) disappears and the fluid moves in the direction of the plate only. The effects of the parameters Ω, M, m on the axial and transverse velocity profiles are shown graphically.

Keywords: Hall effect, thermal radiation, isothermal, vertical plate, mass diffusion, MHD.

1. Introduction
Heat transfer with thermal radiation on convective flows is very important due its significant role in the surface heat transfer. Recent developments in gas cooled nuclear reactors, nuclear power plants, gas turbines, space vehicles, and hypersonic flights have attracted research in this field.
Heat and mass transfer occur simultaneously in processes such as drying, evaporation at the surface of a water body, energy transfer in a wet cooling tower and the flow in a desert cooler. Possible applications of this type of flow can be found in many industries. For example, in the power industry, among the methods of generating electric power is one in which electrical energy is extracted directly from a moving conducting fluid.
The study of magneto hydro dynamic (MHD) plays an important role in agriculture, engineering and petroleum industries. The MHD has also its own practical applications. For instance, it may be used to deal with problems such as the cooling of nuclear reactors by liquid sodium and induction flow meter, which depends on the potential difference in the fluid in the direction perpendicular to the motion and to the magnetic field.
In recent years, the analysis of hydro magnetic flow in the presence of thermal radiation involving heat and mass transfer has attracted the attention of many researchers because of its possible applications in diverse fields of science and technology such as soil sciences, astrophysics, geophysics, nuclear power reactors etc. Magneto hydrodynamics plays a vital role in plasma confinement, liquid-metal cooling of nuclear reactors, electromagnetic casting and also Magnetic Drug Targeting.
Hall Effect plays a vital role in the field of science and technology such as Hall effect sensors are used in rotating speed sensors, fluid flow sensors, current sensors and pressure sensors. Brushless DC motors based on motion sensing uses the principle of Hall Effect. Hall effect joysticks find its application in mining trucks, cranes, diggers, scissor lifts. Hall effect thruster is used to propel spacecraft. Using the principles of magnetic flux leakage, hall probes are used to measure magnetic fields, inspect pipelines.
Free convection effects on the MHD Stokes problem for a vertical plate were carried out by Soundalgekar *et al* [1]. An exact solution for unsteady magneto hydrodynamic free convection flow with constant heat flux was studied by Sacheti *et al* [2]. The effect of Hall currents on the magneto hydrodynamic boundary layer flow past a semi – infinite flat plate was given by Katagiri [3]. Hall effects on MHD flow past an accelerated plate was studied by Dekha [4]. Hall effects on hydromagnetic free convection flow along a porous flat plate with mass transfer were given by Hossian *et al* [5]. Hall effects on magneto hydrodynamic free convection about a semi – infinite vertical flat plate were given by Pop *et al* [6]. Hall effects on magneto hydrodynamic boundary layer flow over a continuous moving flat plate was given by Pop *et al* [7]. Investigations on Hall effects in a rotating system by were given by Dileep Singh Chauhan *et al* [8]. Heat and mass transfer in MHD free convection flow over an inclined plate with Hall current were given by Mohammad Shah Alam *et al* [9]. MHD transient flow with Hall current past an accelerated horizontal porous plate in a rotating system was given by Nazibuddin Ahmed *et al* [10]. Sarkar *et al* [11] considered Hall effects on moving vertical plate and concluded that fluid velocity, temperature raises due to viscous and joule dissipations. Effects of Hall current on a sheet which is exponentially stretching in radius, in cylindrical co-ordinates using homotopy analysis was carried out by Haider Zaman *et al* [12].

Muthucumaraswamy *et al* [13] solved for a Hall effect problem with velocity profiles. Thamizhsudar *et al* [14] extended the problem of Hall effects on an exponentially accelerated vertical plate without chemical reaction and radiation.
The objective of this work is to study the thermal radiation effects on flow past an parabolic accelerated isothermal vertical plate in the presence of magnetic field and Hall currents, whenever the plate is cooled. Skin friction is also discussed.

2. Mathematical Analysis

Initially, the plate and the fluid are in stationary medium and with same temperature. Here, the x' -axis is taken along the vertical plate in the vertically upward direction and the y' -axis is taken normal to the plate. Initially the plate and the fluid were rotating with a constant angular velocity Ω' about the z' -axis normal to the plate, which is perpendicular to x' -axis and y' -axis. Here the unsteady flow of a viscous incompressible fluid past an parabolic accelerated isothermal verticle plate with uniform mass diffusion is considered. A magnetic field of uniform strength B_0 is applied transversely to the plate. At time $t' \le 0$, the plate and the fluid are maintained at the same constant temperature T'_∞ and concentration of the fluid is C'_∞. At time $t' > 0$, the plate is parabolic accelerated with a velocity $u = u_0 t'^2$ in its own plane against gravitational field. At time $t' > 0$, temperature of the plate and the concentration level near the plate is raised linearly with respect to time. That is the temperature of the plate is raised to T'_w and the concentration level is raised to C'_w.

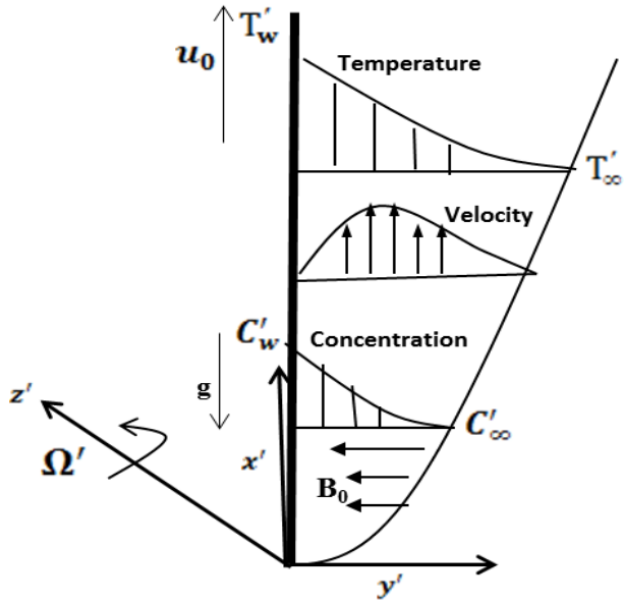

Flow model of the problem

By usual Boussinesq's approximation, the unsteady flow is governed by the following:
Momentum Equation:

$$\frac{\partial u}{\partial t'} = \upsilon \frac{\partial^2 u}{\partial z'^2} + 2\Omega' v - \frac{\sigma \mu_e^2 B_0^2}{\rho\left(1+m^2\right)}\left(u + mv\right) + g\beta\left(T' - T'_\infty\right) + g\beta^*\left(C' - C'_\infty\right) \tag{1}$$

$$\frac{\partial v}{\partial t'} = \upsilon \frac{\partial^2 v}{\partial z'^2} - 2\Omega' u + \frac{\sigma \mu_e^2 B_0^2}{\rho\left(1+m^2\right)}\left(mu - v\right) \tag{2}$$

Energy Equation:

$$\rho C_p \frac{\partial T'}{\partial t'} = k \frac{\partial^2 T'}{\partial z^2} - \frac{\partial q_r}{\partial z} \tag{3}$$

Mass diffusion Equation:

$$\frac{\partial C'}{\partial t'} = D\frac{\partial^2 C'}{\partial z^2} \tag{4}$$

Where u is the axial velocity and v is the transverse velocity.
The initial and boundary conditions are

$$t' \le 0 : u = 0,\ v = 0,\ T' = T'_\infty,\ C' = C'_\infty \text{ for all z}$$
$$t' > 0 : u = u_0 t'^2,\ v = 0,\ T' = T'_w,\ C' = C'_w \text{ at z=0}$$
$$t' > 0 : u \to 0,\ v \to 0,\ T' \to T'_\infty,\ C' \to C'_\infty \text{ as } z \to \infty \tag{5}$$

The local radiant for the case of an optically thin gray gas is expressed by

$$\frac{\partial q_r}{\partial z} = -4a^*\ \sigma(T'^4_\infty - T'^4) \tag{6}$$

It is assumed that the temperature differences within the flow are sufficiently small such that T'^4 may be expressed as a linear function of the temperature. This is accomplished by expanding T'^4 in a Taylor series about T'_∞ and neglecting higher-order terms, thus

$$T'^4 \cong 4T'^3_\infty\ T' - 3T'^4_\infty \tag{7}$$

By using equations (6) and (7), equation (3) reduces to

$$\rho\, C_p\ \frac{\partial T'}{\partial t'} = k\ \frac{\partial^2 T'}{\partial y^2} + 16a^*\sigma T'^3_\infty\ (T'_\infty - T') \tag{8}$$

On introducing non-dimensional quantities:

$$U = u\left(\frac{u_0}{\nu^2}\right)^{\frac{1}{3}},\ t = \left(\frac{u_0^{\,2}}{\nu}\right)^{\frac{1}{3}} t',\ Z = z'\left(\frac{u_0}{\nu^2}\right)^{\frac{1}{3}},$$

$$\mathrm{M} = \frac{\sigma B_0^{\,2}}{\rho}\ \left(\frac{\nu}{u_0^{\,2}}\right)^{\frac{1}{3}}, Gc = \frac{g\beta(C'-C'_\infty)}{(\nu.u_0)^{1/3}},\ Gr = \frac{g\beta(T-T_\infty)}{(\nu.u_0)^{1/3}},$$

$$R = \frac{16a^*\sigma.T_\infty^{\,3}}{k}\left(\frac{\nu^2}{u_0}\right)^{\frac{2}{3}},\ C = \frac{C'-C'_\infty}{C'_W - C'_\infty},\quad \theta = \frac{T'-T'_\infty}{T'_W - T'_\infty},\quad \mathrm{Pr} = \frac{\mu C_p}{K},\quad Sc = \frac{\upsilon}{D},\ \Omega = \Omega'\left(\frac{\nu}{u_0^{\,2}}\right)^{\frac{1}{3}}$$

Equations (1) to (5) are reduced to the non-dimensional form as:

$$\frac{\partial U}{\partial t} = \frac{\partial^2 U}{\partial Z^2} + 2\Omega V - \frac{2M^2}{1+m^2}(U + mV) + Gr\theta + GcC \tag{9}$$

$$\frac{\partial V}{\partial t} = \frac{\partial^2 V}{\partial Z^2} - 2\Omega U + \frac{2M^2}{1+m^2}(mU - V) \tag{10}$$

$$\frac{\partial \theta}{\partial t} = \frac{1}{\mathrm{Pr}}\frac{\partial^2 \theta}{\partial Z^2} - \frac{R}{\mathrm{Pr}}\theta \tag{11}$$

$$\frac{\partial C}{\partial t} = \frac{1}{Sc}\frac{\partial^2 C}{\partial Z^2} \tag{12}$$

The initial and boundary conditions in non-dimensional form are

$$t' \le 0 :\ U = 0, V = 0,\ \theta = 0, C = 0 \text{ for all Z}$$

$$t > 0: U = t^2,\ V = 0,\ \theta = 1,\ C = 1 \text{ at } Z = 0$$
$$t > 0: U \to 0,\ V \to 0,\ \theta \to 0,\ C \to 0 \text{ as } Z \to \infty \quad (13)$$

The above equations (9)-(12) and the boundary conditions (13) can be combined as

$$\frac{\partial F}{\partial t} = \frac{\partial^2 F}{\partial Z^2} - aF + G_r\theta + G_c C \quad (14)$$

$$\frac{\partial \theta}{\partial t} = \frac{1}{\Pr}\frac{\partial^2 \theta}{\partial Z^2} - \frac{R}{\Pr}\theta \quad (15)$$

$$\frac{\partial C}{\partial t} = \frac{1}{Sc}\frac{\partial^2 C}{\partial Z^2} \quad (16)$$

Where $a = \frac{2M^2}{1+m^2} + 2i\left[\Omega - \frac{M^2 m}{1+m^2}\right]$

With boundary conditions

$$t' \le 0: F = 0,\ \theta = 0,\ C = 0 \text{ for all Z}$$
$$t > 0: F = t^2,\ \theta = 1,\ C = 1 \text{ at } Z = 0$$
$$t > 0: F \to 0,\ \theta \to 0\ C \to 0 \text{ as } Z \to \infty \quad (17)$$

Where F=U+iV, U represents the axial velocity(primary velocity), V represents the transverse velocity(secondary velocity). All the physical variables are defined in the nomenclature.

2. Discussion of Solution

Equations (14) to (16), subject to the boundary conditions (17), are solved by the usual Laplace-transform technique and the solutions are derived as follows:

$$\theta(z,t) = \frac{1}{2}\left[\exp(2\eta\sqrt{Rt})\,erfc(\eta\sqrt{\Pr} + \sqrt{bt}) + \exp(-2\eta\sqrt{Rt})\,erfc(\eta\sqrt{\Pr} - \sqrt{bt})\right] \quad (18)$$

$$C(z,t) = erfc(\eta\sqrt{Sc}) \quad (19)$$

$$F(z,t) = \left\{\begin{array}{l}\left[\frac{\eta^2 t}{a} + t^2\right]S + \left[\frac{1}{4a} - t\right]2\eta\sqrt{t}T - \frac{\eta t}{a\sqrt{\pi}}\exp(-\eta^2 - at) + (e+f)A_1 \\ -e\exp(ct)A_2 - f\exp(dt)A_3 - eA_4 + e\exp(ct)A_5 - fA_6 + f\exp(dt)A_7\end{array}\right\} \quad (20)$$

Where

$$S = \frac{1}{2}\left[\exp(2\eta\sqrt{Mt})\,erfc(\eta + \sqrt{Mt}) + \exp(-2\eta\sqrt{Mt})\,erfc(\eta - \sqrt{Mt})\right]$$

$$T = \frac{1}{2\sqrt{M}}\left[\exp(-2\eta\sqrt{Mt})\,erfc(\eta - \sqrt{Mt}) - \exp(2\eta\sqrt{Mt})\,erfc(\eta + \sqrt{Mt})\right]$$

$$A_1 = \exp(2\eta\sqrt{at})\,erfc(\eta + \sqrt{at}) + \exp(-2\eta\sqrt{at})\,erfc(\eta - \sqrt{at})$$

$$A_2 = \exp(2\eta\sqrt{(a+c)t})\,erfc(\eta + \sqrt{(a+c)t}) + \exp(-2\eta\sqrt{(a+c)t})erfc(\eta - \sqrt{(a+c)t})$$

$$A_3 = \exp(2\eta\sqrt{(a+d)t})\,erfc(\eta + \sqrt{(a+d)t}) + \exp(-2\eta\sqrt{(a+d)t})erfc(\eta - \sqrt{(a+d)t})$$

$$A_4 = \exp(2\eta\sqrt{Rt})erfc(\eta\sqrt{Pr} + \sqrt{bt}) + \exp(-2\eta\sqrt{Rt})erfc(\eta\sqrt{Pr} - \sqrt{bt})$$

$$A_5 = \exp(-2\eta\sqrt{Pr(c+b)t})\,erfc(\eta\sqrt{Pr} - \sqrt{(c+b)t}) + \exp(2\eta\sqrt{Pr(c+b)t})erfc(\eta\sqrt{Pr} + \sqrt{(c+b)t})$$

$$A_6 = erfc(\eta\sqrt{Sc})\ A_7 = \exp(-2\eta\sqrt{Scdt})\,erfc(\eta\sqrt{Sc} - \sqrt{dt}) + \exp(2\eta\sqrt{Scdt})erfc(\eta\sqrt{Sc} + \sqrt{dt})\Big]$$

where

$$b=\frac{R}{Pr},\ c=\frac{R-a}{1-Pr},d=\frac{a}{Sc-1},e=\frac{Gr}{2c(1-Pr)}\ \ f=\frac{Gc}{2d(1-Sc)}$$

erfc is the complementary error function.

In order to get the physical insight into the problem, the numerical values of F have been computed from (20). While evaluating this expression, it is observed that the argument of the error function is complex and, hence, we have separated it into real and imaginary parts by using the following formula:

$$erf(a+ib)=erf(a)+\frac{\exp(-a^2)}{2a\pi}\left[1-\cos(2ab)+i\sin(2ab)\right]\ \ +\frac{2\exp(-a^2)}{\pi}\sum_{n=1}^{\infty}\frac{\exp(-\frac{n^2}{4})}{n^2+4a^2}\left[f_n(a,b)+ig_n(a,b)\right]$$

Where

$$f_n=2a-2a\cosh(nb)\cos(2ab)+n\sinh(nab)\sin(2ab)$$

and

$$g_n=2a\cosh(nb)\sin(2ab)+n\sinh(nab)\cos(2ab)\qquad \left|\in(a,b)\right|\approx 10^{-16}\left|erf(a+ib)\right|$$

3. Skin Friction

Skin friction from velocity field in non-dimensional form is given by

$$\tau=\left(\frac{\partial F}{\partial Z}\right)_{Z=0}$$

From equations (20) we have

$$\tau = -(t^2+2e+2f)\{\sqrt{a}\ \text{erf}(\sqrt{at}\ )+\frac{1}{\sqrt{\pi t}}\exp(-at)\}$$

$$+\frac{1}{\sqrt{a}}\ (\frac{1}{4a}\text{-t})\ \text{erf}(\sqrt{at}\ )-\frac{\sqrt{t}}{2a\sqrt{\pi}}\exp(-at)+$$

$$2\text{fexp(dt)}\{\sqrt{a+d}\ \text{erf}(\sqrt{(a+d)t}\ )+\frac{1}{\sqrt{\pi t}}\exp(-(a+d)t)\}+$$

$$2\text{eexp(ct)}\{\sqrt{a+c}\ \text{erf}(\sqrt{(a+c)t}\ )+\frac{1}{\sqrt{\pi t}}\exp(-(a+c)t)\}+2\text{e}\{\sqrt{R}\ \text{erf}(\sqrt{bt}\ )$$

$$+\frac{\sqrt{\text{Pr}}}{\sqrt{\pi t}}\exp(-bt)$$

$$\}-2\text{fexp(ct)}\{\sqrt{\text{Pr}(b+c)}\ \text{erf}(\sqrt{(b+c)t}\ )+\frac{\sqrt{\text{Pr}}}{\sqrt{\pi t}}\exp(-(b+c)t)\}+2\text{f}$$

$$\{\frac{\sqrt{Sc}}{\sqrt{\pi t}}\}-2\text{fexp(dt)}\{\sqrt{dSc}\ \text{erf}(\sqrt{dt}\ )+\frac{\sqrt{Sc}}{\sqrt{\pi t}}\exp-(dt)\}$$

$\tau_x=-\left[\frac{\partial U}{\partial Z}\right]_{Z=0}$ is the skin friction due to axial velocity and

$\tau_y=-\left[\frac{\partial V}{\partial Z}\right]_{Z=0}$ is the skin friction due to transverse velocity

$$b=\frac{R}{\text{Pr}}c=\frac{R-a}{1-Pr},d=\frac{a}{Sc-1},e=\frac{Gr}{2c(1-Pr)}$$

erfc is the complementary error function.

4. Profiles for Concentration, velocity(axial and transverse), temperature and skin friction

To plot the profiles, it is considered that Prandtl number (Pr) as 0.71.

Figure 1 depicts the concentration profiles for Hydrogen (0.16), Water vapour (0.6), Ethyl Benzene (2.01). Schmidt number (Sc) gives the relationship between momentum diffusitivity and mass diffusitivity. Concentration in the presence of Ethyl Benzene is less when compared to Hydrogen, and Water vapour. Concentration boundary layer decreases for increasing values of Schmidt number. The temperature profiles are calculated for different values of thermal radiation parameter ($R = 2,5,10$) are shown in figure 2. for air ($Pr = 0.71$). The effect of thermal radiation parameter is important in temperature profiles. It is observed that the temperature profiles increases with decreasing radiation parameter.

Greater cooling of the surface results in an increase in the velocity. Mass and thermal buoyancy effect increases as there is an increase in thermal grashof number. This increases the speed of the flow. Figure 3 clearly shows that, an increase in thermal and mass grashof number (Gr and Gc) results in decrease in axial velocity. From Figure 4, it is seen that, for increasing values of Gr and Gc, the transverse velocity decreases.

From figure 5, it is clear that there is a decrease in axial velocity when there is an increase in thermal radiation parameter and figure 6 shows that there is an increase in transverse velocity when the thermal radiation parameter increases.

Figure 7 and Figure 8 clearly shows that skin friction due to primary velocity($\boldsymbol{\tau_x}$) increases for increasing values of thermal radiation parameter (R) and also increases for increasing values of Gr and Gc respectively. Figure 9 and Figure 10 shows that skin friction due to secondary velocity($\boldsymbol{\tau_Y}$) decreases for increasing values of thermal radiation parameter (R), and also decreases for increasing values of Gr and Gc respectively.

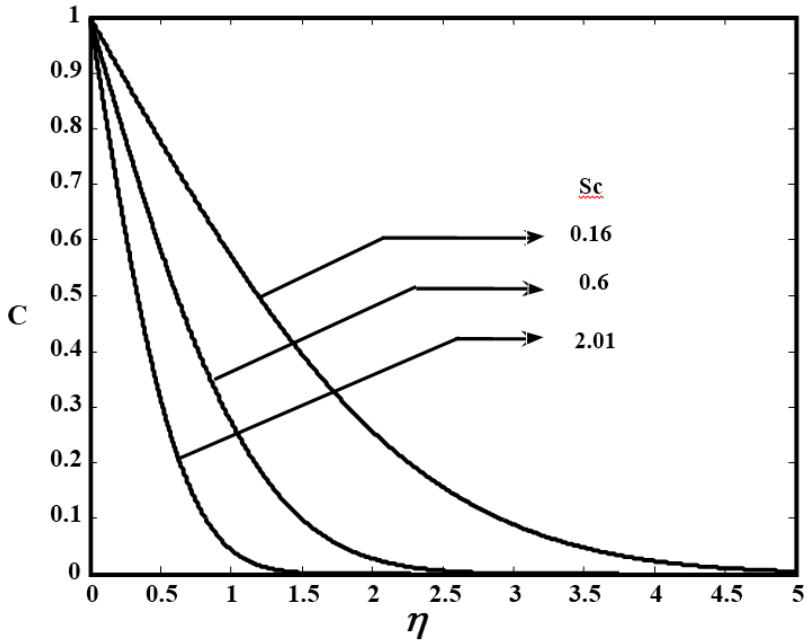

Fig 1: Concentration profiles for different values of Sc

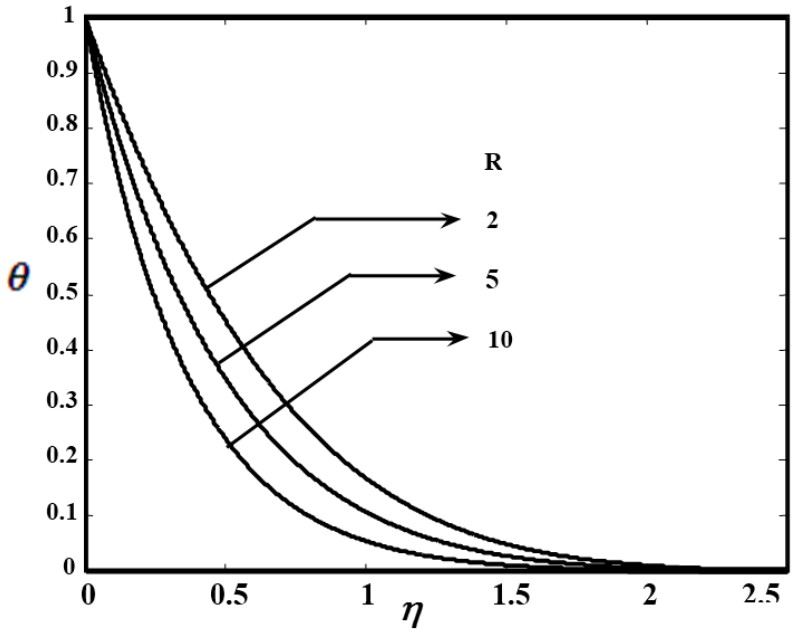

Fig 2: Temperature profiles for different values of R

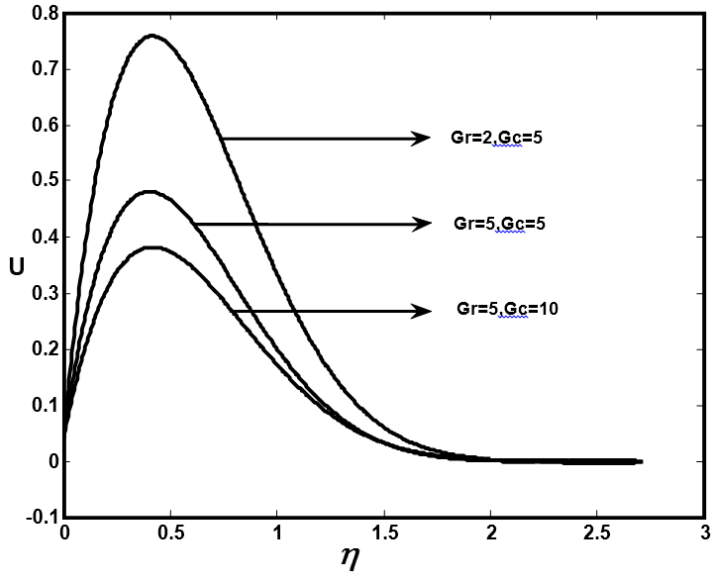

Fig 3: Axial velocity profiles for different values of Gr and Gc

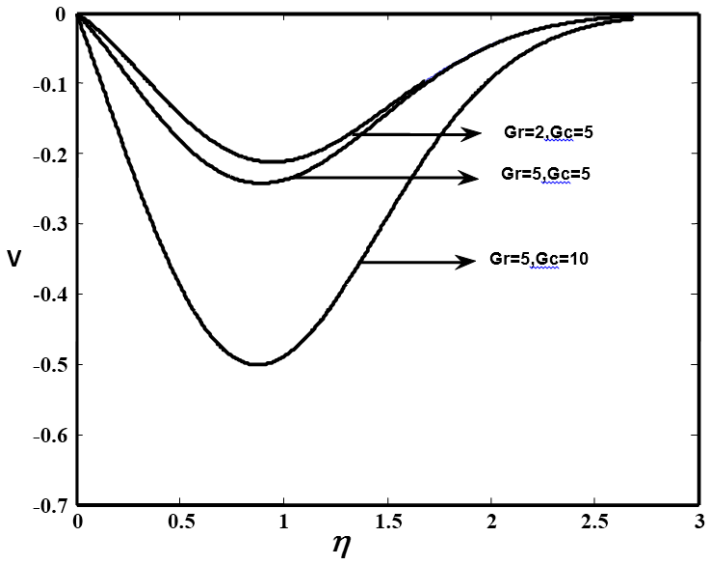

Fig 4: Transverse velocity profiles for different values of Gr and Gc

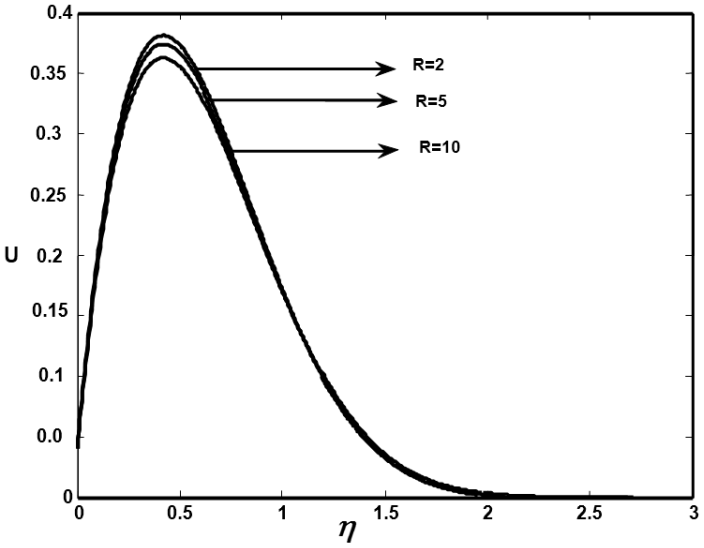

Fig 5: Axial velocity profiles for different values of R

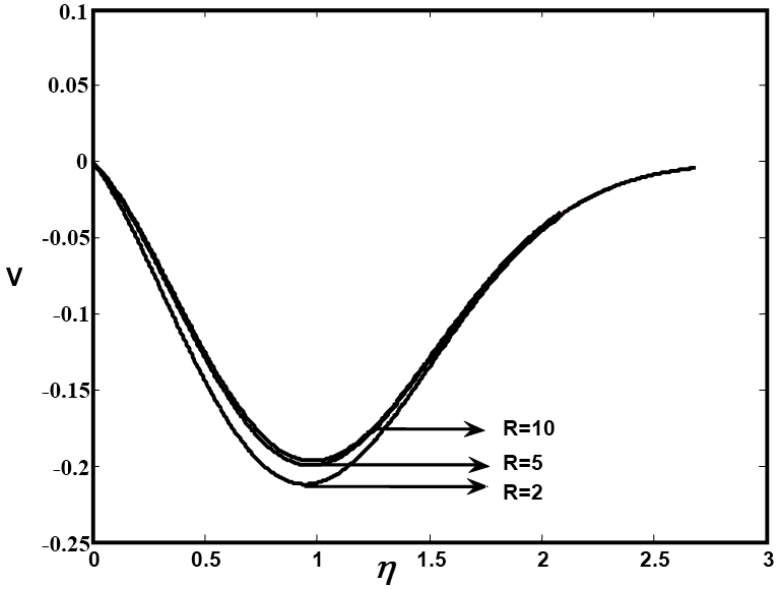

Fig 6: Transverse velocity profiles for different values of R

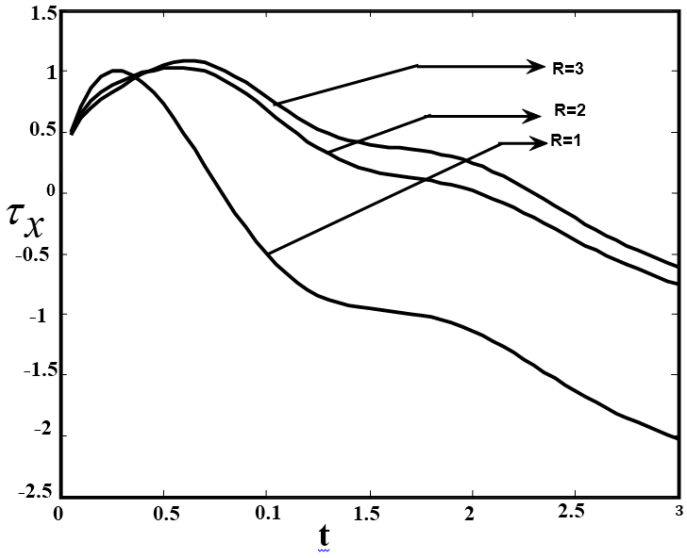

Fig 7: Primary Skin friction profiles for different values of R

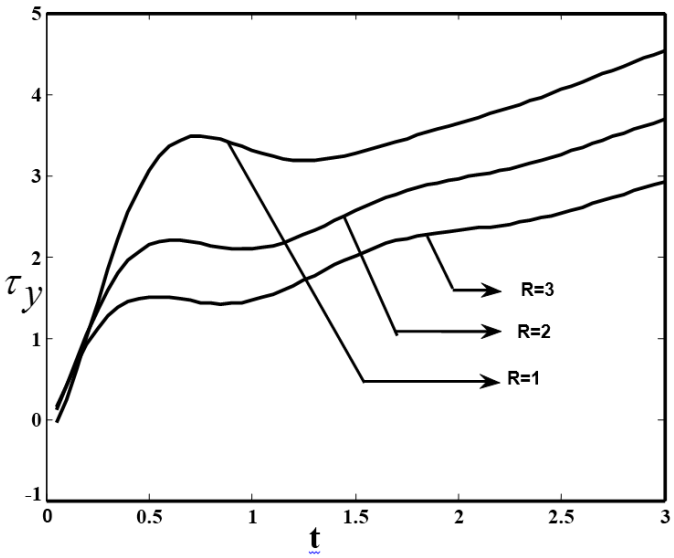

Fig 8: Secondary Skin friction Profiles for different values of R

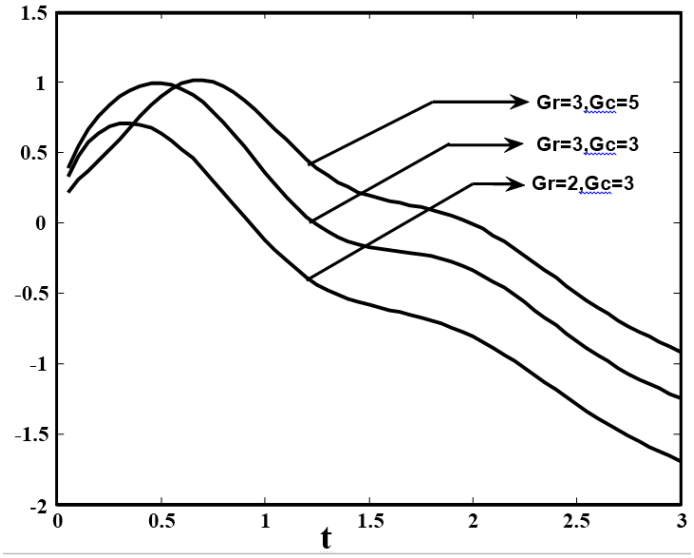

Fig 9: Primary Skin Friction Profiles for different values of Gr and Gc

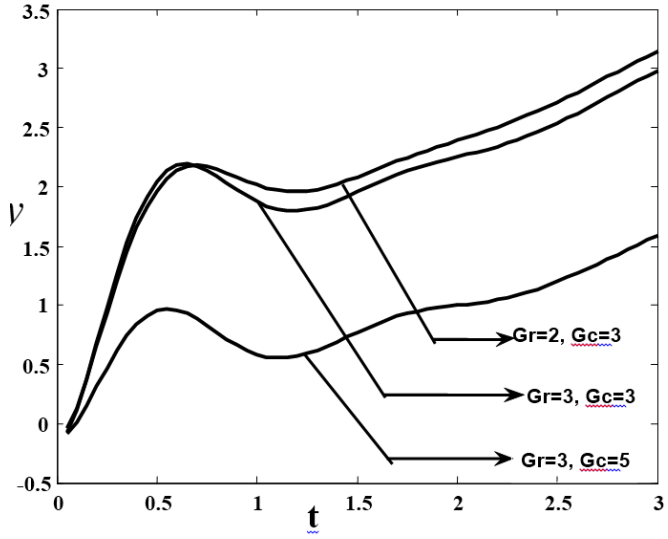

τ_x

Fig 10: Secondary Skin Friction Profiles for different values of Gr and Gc

5. Conclusion

An analytical study of profiles for concentration, temperature, axial velocity, transverse velocity and skin friction on convective flow past a parabolic accelerated vertical plate in the presence of Magnetic field, Hall current and thermal radiation has been carried out. The case of cooling of the plate (Gr > 0, Gc > 0) as convection currents are carried from the plate is focused. It is observed that

(i) Concentration(C) decreases for increasing values of Schmidt number (Sc).

(ii) Axial velocity(U)
   (a) decreases for increasing values of thermal grashof number and mass grashof number (Gr and Gc).
   (b) decreases for increasing values of thermal radiation parameter (R).

(iii) Transverse velocity(V)
   (a) increases only for increasing values of thermal radiation parameter (R).
   (b) decreases for increasing values of thermal grashof number (Gr), mass grashof number(Gc).

(iv) Skin friction due to primary velocity (τ_x)
   (a) increases for increasing values of thermal radiation parameter (R).
   (b) increases for increasing for increasing values of thermal grashof number (Gr), mass grashof number(Gc).

(v) Skin friction due to secondary velocity (τ_y)
   (a) decreases for increasing values of thermal radiation parameter (R).
   (b) decreases for increasing values of thermal grashof number (Gr), mass grashof number(Gc).

6. References

1. Soundalgekar VM, Gupta SK, Aranake RN. Free convection effects on the MHD Stokes problem for a vertical plate, Nuclear Engineering and Design. 1979; 51(3):403-407.
2. Sacheti NC, Chandran P, Singh AK. An exact solution for unsteady magnetohydrodynamic free convection flow with constant heat flux, International Communications in Heat and Mass Transfer. 1986; 29:1465-1478.
3. Katagiri M. The effect of Hall currents on the magnetohydrodynamic boundary layer flow past a semi – infinite flat plate. J Phys Soc Japan. 1969; 27:1051-1059.
4. Deka RK. Hall effects on MHD flow past an accelerated plate, Theoret. Appl. Mech. 2008; 35:333-346.
5. Hossain MA, Rashid RIMA. Hall effects on hydromagnetic free convection flow along a porous flat plate with mass transfer. J Phys Soc Japan. 1987; 56:97-104.
6. Pop I, Watanabe T. Hall effects on magnetohydrodynamic free convection about a semi – infinite vertical flat plate, Int. J Eng Sci. 1994; 32:1903-1911.
7. Pop I, Watanabe T. Hall effects on magnetohydrodynamic boundary layer flow over a continuous moving flat plate, Acta Mech. 1995; 108:35-47.
8. Dileep Singh Chauhan, Priyanka Rastogi. Hall effects on MHD slip flow and heat transfer through a porous medium over an accelerated plate in a rotating system. 2012; 14:228-236.
9. Mohammad Shah Alam, Mohammad Ali, Delowar Hossain Md. Heat and mass transfer in MHD free convection flow over an inclined plate with Hall curren. The International Journal of Engineering and Science. 2013; 2:81-88.
10. Nazibuddin Ahmed, Jiwan Krishna Goswami, Dhruba Prasad Barua. MHD transient flow with Hall current past an accelerated horizontal porous plate in a rotating system. Open journal of fluid dynamics. 2013; 3:278-285.
11. Sarkar BC, Das S, Jana RN. Hall effects on unsteady MHD free convective flow past an accelerated moving vertical plate with viscous and joule dissipations. International journal of computer applications. 2013; 70:19-28.
12. Haider Zaman, Arif Sohail, Azhar Ali, Tarique Abbas. Effects of hall current on flow of unsteady MHD axisymmetric second-grade fluid with Suction and blowing over an exponentially Stretching sheet. Open Journal of Modelling and Simulation. 2014; 2:23-33.
13. Muthucumaraswamy R, Thamizhsudar M, Pandurangan J. Hall effect on MHD flow past an exponentially accelerated vertical plate in the presence of rotation", Annals of faculty Engineering Hunedoara, Tome XII-Fascicule 3. 2014.
14. Thamizhsudar M, Pandurangan J. Hall effects on magneto hydrodynamic flow past an exponentially accelerated vertical plate in a rotating fluid with mass transfer effects. Elysium journal research and management. 2014; 1:143-149.